Influence of Type I Collagen Surface Density on Fibroblast Spreading, Motility, and Contractility

Christianne Gaudet, William A. Marganski, Sooyoung Kim, Christopher T. Brown, Vaibhavi Gunderia, Micah Dembo, and Joyce Y. Wong
Department of Biomedical Engineering, Boston University, Boston, Massachusetts 02215

ABSTRACT We examine the relationships of three variables (projected area, migration speed, and traction force) at various type I collagen surface densities in a population of fibroblasts. We observe that cell area is initially an increasing function of ligand density, but that above a certain transition level, increases in surface collagen cause cell area to decline. The threshold collagen density that separates these two qualitatively different regimes, ~160 molecules/μm^2, is approximately equal to the cell surface density of integrin molecules. These results suggest a model in which collagen density induces a qualitative transition in the fundamental way that fibroblasts interact with the substrate. At low density, the availability of collagen binding sites is limiting and the cells simply try to flatten as much as possible by pulling on the few available sites as hard as they can. The force per bond under these conditions approaches 100 pN, approximately equal to the force required for rupture of integrin-peptide bonds. In contrast, at high collagen density adhesion, traction force and motility are limited by the availability of free integrins on the cell surface since so many of these receptors are bound to the surface ligand and the force per bond is very low.

INTRODUCTION

Interactions between cell surface receptors (mostly integrins) and various molecules of the extracellular matrix underlie a wide variety of processes including adhesion, spreading, and motility. In particular, the surface density of adhesive ligand affects the ability of cells to spread, grow, and differentiate (Hansen et al., 1994; Mooney et al., 1992, 1995). In the case of motility, the phenomenon of haptotaxis (Carter, 1967; Dickinson and Tranquillo, 1993; Harris, 1973) clearly demonstrates the ability of cells to sense and respond to the level of a specific surface ligand. Moreover, for a number of cell types and extracellular matrix molecules, cell speed exhibits a biphasic behavior with respect to surface ligand density (DiMilla et al., 1991, 1993; Palecek et al., 1997). Although it also seems obvious that adhesion is important for the generation of cellular traction forces, the details of how traction, spreading, and motility are controlled at different levels of surface ligand have never been directly investigated.

To clarify these matters, we use traction force microscopy (also called the elastic substrate method) to quantify the contractility of BALB/c 3T3 fibroblasts adhered to flexible polyacrylamide substrata that are coated with various densities of type I collagen. This method has previously been used to study the spatial organization and dynamics of cell traction during migration (Beningo et al., 2001; Munevar et al., 2001b; Wang et al., 2001). Furthermore, it has been used to demonstrate that cells can sense and respond to substrate rigidity (Lo et al., 2000), and that H-ras transformation dramatically alters cellular tractions (Munevar et al., 2001a). More recently, other techniques to measure cell traction have been used to quantify the amount of force generated at focal adhesions (Balaban et al., 2001; Tan et al., 2003). In this study, in addition to traction forces, we also make measurements of the projected area and migration speed. We are thus able to follow how independent measures of cell morphology, movement, and force production are modulated by surface collagen density.

Submitted February 3, 2003, and accepted for publication July 23, 2003.

Address reprint requests to Joyce Y. Wong, Dept. of Biomedical Engineering, Boston University, 44 Cummington St., Boston, MA 02215. Tel.: 617-353-2374; Fax: 617-358-0453; E-mail: jywong@bu.edu.

0006-3495/03/11/3329/07 $2.00

MATERIALS AND METHODS

Substrate preparation

Thin films of polyacrylamide are adhered to activated glass coverslips (VWR Scientific, West Chester, PA) according to the procedure described previously (Beningo et al., 2001, 2002; Wang and Pelham, 1998). All substrata used in this study contain 8% acrylamide, 0.04% bis-acrylamide (Bio-Rad, Hercules, CA), and a 1:40 dilution of fluorescent latex beads (0.2 μm; Molecular Probes, Eugene, OR). A 10 μL drop of the solution is placed onto an activated coverslip, flattened with a 12 mm-diameter circular coverslip, and allowed to polymerize at room temperature for 20 min. The desired concentration of calfskin type I collagen (USB, Cleveland, OH) is covalently attached to the polyacrylamide surface using a photoactivatable heterobifunctional linker sulfosuccinimidyl 6 (4-azido-2-nitrophenyl-amino) hexanoate (sulfo-SANPAH; Pierce Biotechnology, Rockford, IL). Sulfo-SANPAH-modified substrata are then incubated with type I collagen at plating concentrations from 0.00075 to 0.8 mg/mL overnight at 4°C.

Substrate characterization

The thickness of the polyacrylamide substrate is estimated to be ~100 μm by vertically focusing a calibrated microscope from the glass surface to the upper surface of the substrate. In addition, the Poisson ratio of polyacrylamide has been previously measured to be ~0.30 (Li et al., 1993). The Young's modulus of the substrate is determined macroscopically using a standard tensile test (Pelham and Wang, 1997). One end of the substrate (dimensions, ~20 × 10 mm) is fixed, and then deformation is induced by attaching known weights at the other end. The Young's modulus can be calculated as $E = (F/A)/(\Delta l/l)$, where F is the applied force, A is the cross-sectional area of the substrate, Δl is the change in length of the substrate, and

l is the original length of the substrate. This method is applied to 10 substrata to obtain a value for the Young's modulus of ~5 kPa. We have also measured the Young's modulus of the substratum using a Hertzian-based microindentation technique (Landau and Lifshitz, 1986), a microneedle technique (Pelham and Wang, 1997), and atomic force microscopy, and found that the values for the Young's modulus agree very well.

Quantifying the attached collagen density

A fibronectin-based assay as described previously (Wong et al., 2003) is utilized to quantify the collagen density attached to the substrata since it is known that fibronectin binds to type I collagen. The basic idea is to bind biotinylated fibronectin to the collagen on the surface of the substrata and then to add streptavidin coupled to horseradish peroxidase to determine the relative amount of collagen based upon changes in the optical density.

Briefly, to minimize effects from the underlying glass surface, the polyacrylamide substrata are cast to cover the entire glass coverslip. Various concentrations of type I collagen are then covalently linked to the upper surface of the substrata using the photoactivatable linker sulfo-SANPAH. After incubation at 4°C overnight, the substrata are washed with distilled water (6 × 15 min) to remove any excess, nonspecifically bound collagen. The substrata are first incubated with 1.5 mL blocking buffer (2% bovine serum albumin (Sigma, St. Louis, MO), 0.05% Tween-20 in 1× phosphate buffered saline) in six-well tissue culture plates (Corning, Corning, NY) for 30 min at 37°C. This is followed by a second incubation with 1.5 mL biotinylated fibronectin (0.2 μg/mL in blocking buffer) for 1 h at 37°C. Fibronectin is biotinylated using biotin hydrazide according to the manufacturer's instructions (Pierce Biotechnology). After rinsing thoroughly with 0.1% Tween-20 in 1× phosphate buffered saline three times, the substrata are incubated with 1.5 mL horseradish peroxidase-streptavidin (Pierce Biotechnology, Rockford, IL) at a dilution of 1:20,000 in blocking buffer for 30 min at 37°C and then thoroughly washed again. Tetramethylbenzidine (Pierce Biotechnology) is then added to the substrata and the color is allowed to develop at room temperature for 10 min. The reaction is stopped with 1.5 mL 1M H_2SO_4, and then 200 μL of the mixture is transferred to a 96-well flat-bottomed ELISA plate (Corning, Corning, NY). The optical density (450 nm) is measured in a microwell plate reader (Opsys MR, Dynex Technologies, Chantilly, VA) to provide a measure of the relative collagen density adhered to the substrata.

To estimate the absolute density of collagen (σ), the same procedure described above is performed on standards that are prepared by drying various known amounts of collagen onto plates at 37°C for 16 h (humidified) and then at 40°C for 24 h (dry). We verified that no collagen is present in the washing solutions removed from the plates during the procedure and, therefore, 100% binding efficiency is assumed. The drying of collagen onto plates has been used previously in conjunction with binding to Sirius red to quantify collagen concentrations, and 100% binding efficiency was also observed (Walsh et al., 1992).

The absolute density of collagen coupled to the polyacrylamide substrata is calculated from the curve generated from the collagen standards. These results are given in Table 1 and illustrate that σ increases monotonically with the plating concentration. Collagen densities for plating concentrations below 0.025 mg/mL could not be directly detected but are estimated by linear interpolation between the value at 0.025 mg/mL and the origin.

Cell culture and microscopy

BALB/c 3T3 fibroblasts (clone A31, American Type Culture Collection, Manassas, VA) are maintained in Dulbecco's modified Eagle's medium supplemented with 50 μg/mL penicillin, 50 U/mL streptomycin, 200 mM L-glutamine (Invitrogen, Carlsbad, CA), and 10% calf serum (Hyclone, Logan, UT). Cells are plated onto collagen-coated polyacrylamide substrata at a density of 1000 cells/cm^2 to avoid cell-cell contacts. After 15–18 h of incubation, the substrata are mounted on a Zeiss Axiovert S 100 microscope (Zeiss, Thornwood, NY) equipped with a Zeiss 40X, NA 0.75 phase objective, a motorized stage (model 99D008-Z1, Ludl, Hawthorne, NY), and a stage incubator that keeps the environment at 37°C and 5% CO_2. Phase-contrast and fluorescent images are collected using a cooled CCD camera (Princeton Instruments, Trenton, NJ) and the Metamorph imaging software (Universal Imaging, Downingtown, PA). Imaging media consisting of Leibovitz's L-15 media (Invitrogen) and 10 mM HEPES buffer supplemented with calf serum, L-glutamine, and penicillin-streptomycin are used to maintain the pH at ~7.4.

TABLE 1 Relationship between plating concentration and attached surface density (σ) of type I collagen

Plating concentration (mg/mL)	σ* (molecules/μm^2)	N ($\|\|\mathbf{T}\|\|$ and $\|\|\mathrm{A}\|\|$)	N ($\|\|\mathbf{S}\|\|$)
0.00075	4.8	12	–
0.001	6.4	8	–
0.0025	16	18	–
0.0075	48	8	–
0.015	96	9	35
0.025	160	15	40
0.05	250	–	26
0.075	340	23	–
0.15	450	–	39
0.2	470	75†	–
0.4	580	59‡	22
0.8	750	24	14

The sample size at each concentration is indicated by N.
*Calculated using an MW (type I collagen) = 350,000 g/mol.
†Data combines three plating concentrations, 0.1, 0.15, and 0.2 mg/mL (430, 450, and 470 molecules/μm^2).
‡Data combines two plating concentrations, 0.3 and 0.4 mg/mL (525 and 580 molecules/μm^2).

Determination of cell motility

Time-lapse microscopy equipped with a motorized stage (Ludl model 99D008-Z1) is used to capture phase-contrast images of single cells at 15 min intervals up to 20 h. Fields are chosen at random and cells that come into contact with each other are not analyzed. Mean-squared displacements of the centroid of each cell are calculated using the Metamorph imaging software. Each cell is classified either as motile or immotile according to the criterion described by DiMilla et al. (1992). The speed (S) and persistence time (P) of each motile cell are obtained by fitting the mean-squared displacement ($\langle d^2 \rangle$) as a function of time (t) to a random walk model equation $\langle d^2 \rangle = 2S^2P[t - P(1 - \exp(-t/P))]$ (DiMilla et al., 1992; Dunn, 1983). Note that the Levenberg-Marquandt method for nonlinear least-squares fitting is used to obtain S and P.

Measurement of cell contractility

Cell traction forces are determined using the traction force microscopy method as developed by Dembo and co-workers (Dembo et al., 1996; Dembo and Wang, 1999). Briefly, fluorescent images of the substrate are recorded to capture the marker beads in the stressed state. In addition, phase-contrast images are acquired to record the morphology of the cell. Trypsin (Invitrogen) is then added to disrupt cell-substrate interactions and cause cell detachment. A final fluorescent image of the substrate is taken to capture the marker beads in the relaxed, unstressed state.

Deformations of the substrate in the region surrounding a cell are determined using a correlation-based optical flow algorithm (Marganski et al., 2003). Essentially, a small patch that contains a number of marker beads is defined within the fluorescent image of the relaxed, unstressed substrate. Then a search is performed within the fluorescent image of the stressed substrate for a patch with the most similar intensity pattern.

Deformation vectors are then constructed from the center of the patch within the unstressed substrate to the center of the patch within the stressed substrate that was determined to be the best match. Multiple measurements can be performed in a similar manner to provide a robust estimation of the substrate deformation field. Interpolation methods are used to refine the measurements to an accuracy of ~0.10 pixel.

The theory for converting deformations of elastic substrata into a traction field has been previously described (Dembo et al., 1996; Dembo and Wang, 1999). Briefly, it is assumed that the substrate behaves as a semi-infinite, isotropic half-space and that all forces act tangentially along the surface of the substrate, are confined within the cell boundary, and are constrained such that the net forces and torques are zero. The coordinate system of the traction field is constructed by tracing the cell boundary and tessellating the region enclosed with a mesh of quadrilaterals. The corner of each quadrilateral represents a discrete spatial coordinate at which an individual traction vector is defined. The area of the cell ($|A|$) is computed by numerical integration over the mesh using four-point Gaussian quadrature. The most likely traction field is computed by maximizing a Bayesian likelihood function that provides the best approximation to the substrate deformations.

An overall measure of cellular contractility is obtained by computing the total absolute force as $|F| = \iint \sqrt{T_x^2(x,y)+T_y^2(x,y)}\,dx\,dy$, where $\mathbf{T}(x,y) = [T_x(x,y), T_y(x,y)]$ is the continuous field of traction vectors defined at any spatial position (x,y) within the cell. Dividing $|F|$ by the cell area ($|A|$) yields the average traction magnitude ($|\mathbf{T}|$), which is just a measure of the average absolute force per unit area exerted within the cell.

RESULTS

Cell-to-cell variability in contractility and area

Data generated during a typical traction force experiment are depicted in Fig. 1. Here a BALB/c 3T3 fibroblast with $|A| \approx 1200\ \mu m^2$ is adhered to a polyacrylamide substrate with $\sigma \sim 470\ \mu m^{-2}$ (Fig. 1 *A*). The substrate deformation field due to the activity of the cell is shown in Fig. 1 *B*. The length and direction of each vector indicate the motion that the substrate undergoes due to the contractility of the cell. The most likely traction field, which explains the substrate deformation data (Fig. 1 *B*), is illustrated in Fig. 1 *D*. The mesh used in making the necessary calculation is shown in Fig. 1 *C*. The average traction magnitude and total absolute force of this cell are $|\mathbf{T}| \sim 3$ kdyn/cm^2 and $|F| \sim 0.04$ dyn, respectively.

Of course, experiments such as those in Fig. 1 must be carried out on a large number of cells to obtain a valid statistical measure of the population behavior at any particular level of collagen. A scatter plot of $|F|$ versus $|A|$ at fixed σ reveals that the cell-to-cell variations in these two quantities are highly correlated. Such plots, for two different collagen densities, are given in Fig. 2. At both collagen densities, there is a linear regression trend with intercept at the origin that is consistent and unbiased over a large range (~10-fold) of the variables. These results can be summarized by saying that regardless of σ, larger cells tend to produce more total force. However, it should be remembered that this is only a correlation. Thus, it could be that stronger cells tend to spread more, or equally well, that larger cells tend to generate more total force.

With the understanding that there is much cell-to-cell variation at any given level of σ, we are nevertheless able to document statistically significant effects of collagen on the average characteristics of the cell population. The qualitative nature of these effects is indicated in Fig. 3, which displays vector plots of the traction field for cells cultured for 15–24 h at four different densities of type I collagen. For each collagen density, the cell shown is selected such that $|A|$ and $|\mathbf{T}|$ are as close as possible to the population averages. In all cases, the traction vectors tend to be centripetal (inwardly directed) and perpendicular to the cell boundary. In cases where the cell is polarized and motile, there are strong tractions at the leading edge. Furthermore, traction is always strongest at the cell periphery and minimal under the nucleus. Obviously, there are very significant differences in both cell area and the overall traction output at different surface densities of collagen.

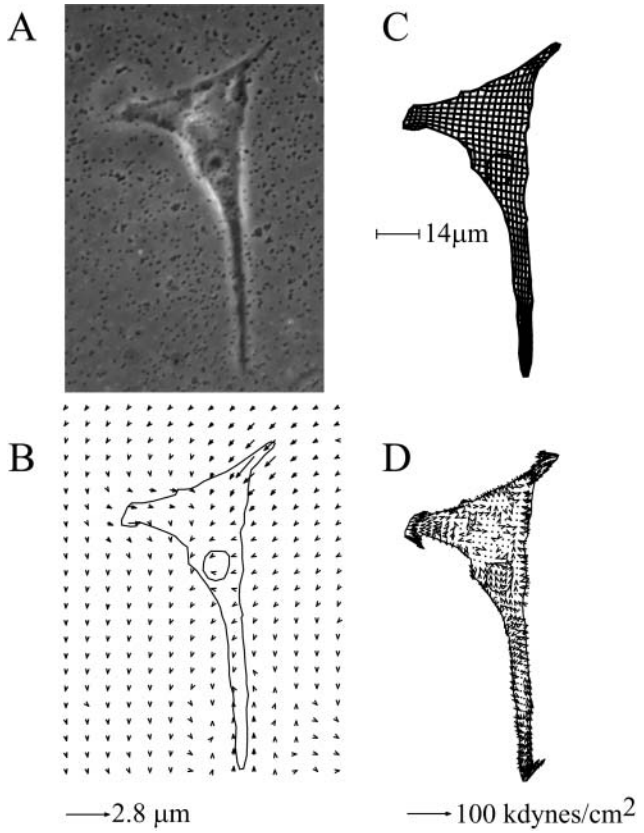

FIGURE 1 Traction force microscopy. (*A*) Phase contrast image of a BALB/c 3T3 fibroblast adhered to a polyacrylamide substrate coated with a type I collagen density of ~470 μm^{-2}. (*B*) Substrate deformation field overlaid on top of the outline of the cell and its nucleus. (*C*) A quadrilateral mesh that defines the traction field coordinate system. (*D*) Most likely traction field that fits the substrate deformation data in *B* and uses the mesh in *C*.

Effect of type I collagen density on the population average of contractility and area

The existence of a linear correlation between $|F|$ and $|A|$ implies that these quantities contain redundant information and that the ratio of these quantities (i.e., $|\mathbf{T}|$) is the most

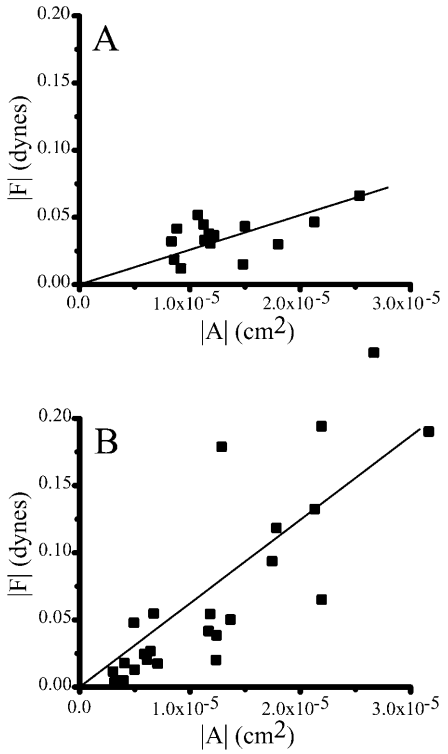

FIGURE 2 Correlation of |A| and |F| for BALB/c 3T3 fibroblasts adhered to substrata coated with σ of (*A*) 160 and (*B*) 470 μm^{-2}. Each set of data is fit linearly through the origin. The slope (kdyn/cm^2) and *R* values for each fit are (*A*) 2.6 and 0.54, and (*B*) 6.0 and 0.84.

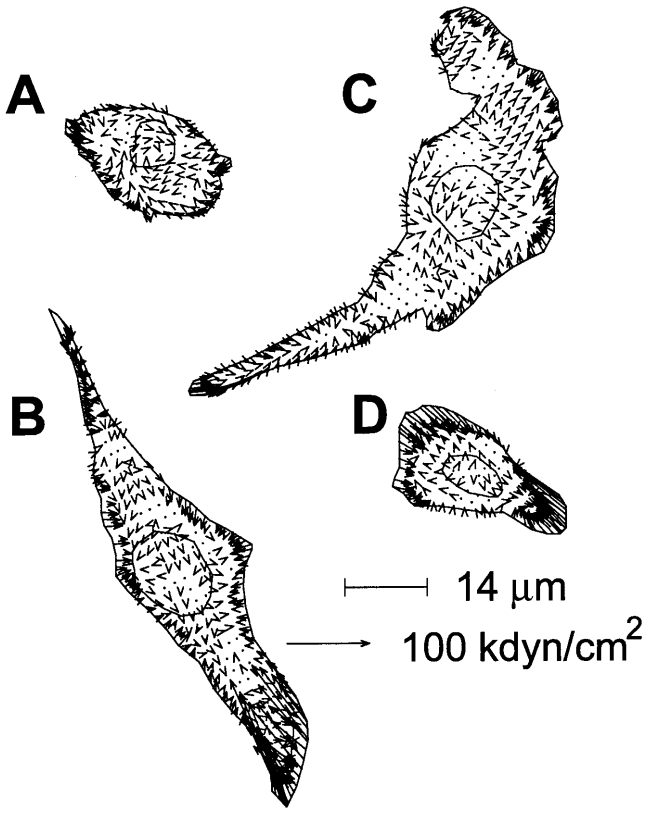

FIGURE 3 Representative traction maps for BALB/c 3T3 fibroblasts adhered to substrata coated with σ of (*A*) 4.8, (*B*) 48, (*C*) 160, and (*D*) 750 μm^{-2}. Cells are selected so that $|\mathbf{T}|$ and |A| are as close as possible to the population averages.

direct statistical measure of the overall contractile response to the substrate independent from any influence of cell size. The slope of the regression line between |F| and |A| provides the population average value of $|\mathbf{T}|$, denoted $\|\mathbf{T}\|$. Fig. 4 *A* shows the value of $\|\mathbf{T}\|$ and the population average of the cell area (denoted $\|A\|$) over the full range of collagen densities studied. The sample size for each data point is indicated in Table 1. There appear to be two regimes in the variation of these variables with collagen density. At lower densities (σ ranging between 5 and 100 μm^{-2}), $\|\mathbf{T}\|$ remains in a restricted range between ~4.4 and ~5.9 kdyn/cm^2, and $\|A\|$ increases monotonically. $\|A\|$ eventually reaches a maximum of ~1300 μm^2 at $\sigma \sim 160\ \mu m^{-2}$, but increasing σ beyond this level causes the qualitative relation of $\|A\|$ and σ to become completely reversed. In other words, $\|A\|$ becomes a decreasing function of σ and eventually decreases by more than a factor of two at the highest collagen density achieved ($\sigma \sim 750\ \mu m^{-2}$). A qualitative shift in the relation of $\|\mathbf{T}\|$ and σ also occurs at an intermediate or transition level of ligand density. In particular, when σ is increased from 100 to 160 μm^{-2}, $\|\mathbf{T}\|$ drops from ~5.9 to ~2.6 kdyn/cm^2. Such a large effect from such a seemingly minor change in the ligand density seems paradoxical given that, in general, one would expect improved opportunities for adhesion to promote rather than retard contractility. It is also notable that this drop in $\|\mathbf{T}\|$ occurs even as $\|A\|$ is increasing to a maximum. Thus, it is difficult to argue that substrata with $\sigma \sim 160\ \mu m^{-2}$ are somehow adverse for cell viability or attachment. Finally, as σ is increased beyond this transition level, $\|\mathbf{T}\|$ becomes an increasing function of ligand density, eventually reaching a value of ~7.0 kdyn/cm^2.

In any event, the dependence of $\|A\|$ and $\|\mathbf{T}\|$ on σ, as shown in Fig. 4 *A*, provides evidence for the idea that when σ exceeds ~160 μm^{-2}, cells tend to undergo a qualitative shift in the way they interact with the substrate. $\|\mathbf{T}\|$ is quite insensitive to σ below the transition level, undergoes a sharp decline near the transition level, and becomes a strongly increasing function of σ above the transition level. In contrast, $\|A\|$ is an increasing function of σ below the transition level, reaches a maximum near the transition level, and becomes a decreasing function of σ above the transition level.

The relationship between the population average total absolute force ($\|F\|$) and σ is shown in Fig. 4 *B*. The sample size for each data point is indicated in Table 1. $\|F\|$ initially increases with increasing σ, undergoes a sharp decrease at $\sigma \sim 160\ \mu m^{-2}$, begins to increase again until σ reaches ~470

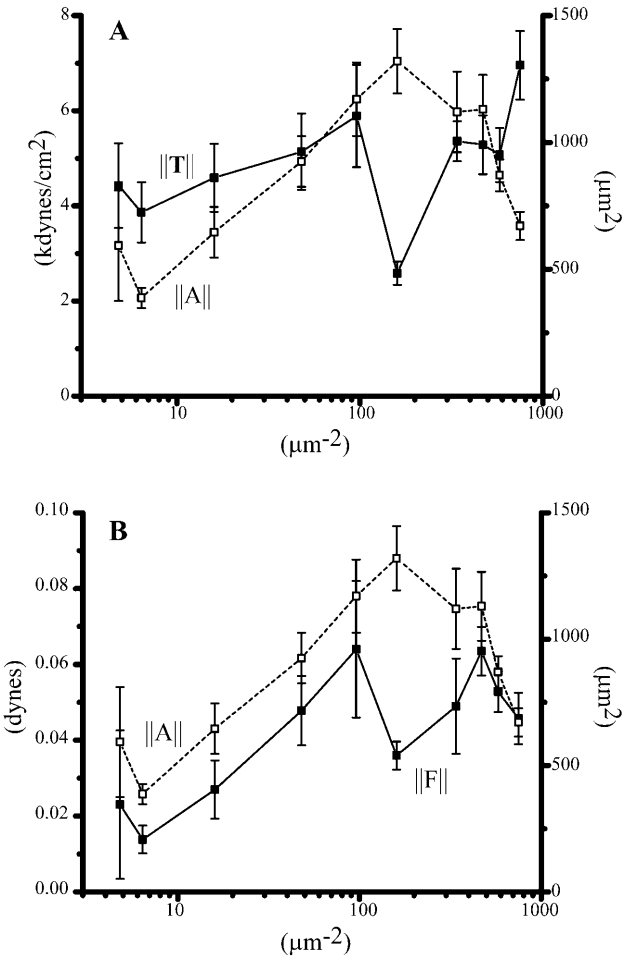

FIGURE 4 Effect of σ on (*A*) $\|\mathbf{T}\|$ and (*B*) $\|F\|$ for the BALB/c 3T3 fibroblast. In both *A* and *B*, ($\|A\|$) is shown. $\|\mathbf{T}\|$ and $\|F\|$ are represented by (■) and $\|A\|$ by (□). Values are reported as an average ± SE. See Table 1 for *n* at each condition.

μm^{-2}, and finally decreases slightly when σ exceeds ~470 μm^{-2}. Overall, the dependence of $\|F\|$ on σ is quite similar to the relationship observed for $\|\mathbf{T}\|$. This is not surprising since $\|F\|$ and $\|\mathbf{T}\|$ are directly related through $\|A\|$.

Effect of type I collagen density on cell migration

The population average cell speed $\|S\|$ also seems to undergo a qualitative change related to σ, but the change seems to be more gradual than what was observed for $\|A\|$ and $\|\mathbf{T}\|$ (Fig. 5). The sample size for each data point is indicated in Table 1. In particular, $\|S\|$ is negligible at ligand densities significantly below the transition level ($\sigma \sim 160\ \mu m^{-2}$). However, near the transition level, a motile phenotype begins to emerge, and $\|S\|$ increases to a maximum of ~10 μm/h at σ ~450 μm^{-2}. Further increases in σ above this level actually decrease motility probably because cells adhere too strongly to the substrate.

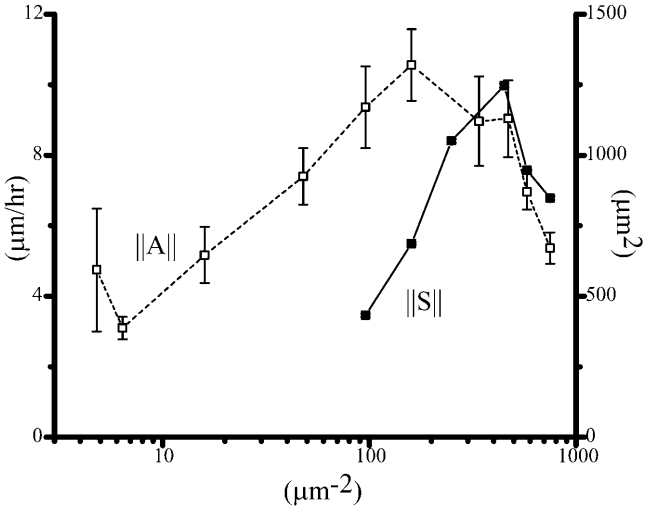

FIGURE 5 Effect of σ on $\|S\|$ and the population average spread area $\|A\|$ for the BALB/c 3T3 fibroblast. $\|S\|$ and $\|A\|$ are represented by (■) and (□), respectively. Values are reported as an average ± SE. See Table 1 for *n* at each condition.

DISCUSSION

At the lowest density of type I collagen examined in this study ($\sigma \sim 5\ \mu m^{-2}$), a typical cell is characterized by the following parameters: $\|A\| \sim 600\ \mu m^2$, $\|F\| \sim 0.025$ dyn, and $\|\mathbf{T}\| \sim 5$ kdyn/cm^2. This means that there are no more than 3000 collagen molecules available for binding, whereas fibroblastic cells express $\sim 5 \times 10^5$ integrin receptors (Akiyama and Yamada, 1985). Assuming that collagen is the limiting factor and that every collagen molecule is bound to a single integrin, we can calculate that a typical integrin-collagen bond is under a tension of ~100 pN. This may be a slight overestimate since there can be up to three integrin binding sites per collagen molecule (Di Lullo et al., 2002). The tension estimated in this fashion can be compared with values derived in two recent studies that used atomic force microscopy to measure the forces needed to break single integrin-RGD bonds (Lee and Marchant, 2001; Lehenkari and Horton, 1999). The loading rates ranged over three orders of magnitude (12 nN/s–37 pN/s), and the force at rupture varied between 30 and 100 pN. The main conclusion is that at low collagen densities, an adherent cell is exerting enormous force through a small number of available linkages and that the force per linkage approaches the limit they can withstand. Presumably, these forces are exerted because the cell senses its rounded morphology and is programmed to try very hard to flatten against the surface as much as possible. Unfortunately, it cannot achieve this objective very well because the adhesive linkages have very short lifetimes, and if the cell were to pull any harder, it would simply tear itself from the surface.

The preceding analysis, by itself, cannot explain why $\|\mathbf{T}\|$ is so insensitive to changes in σ when it is very low (Fig.

4 *A*). However, it is possible to understand this if one considers that the tractions are not uniformly distributed but occur primarily at the cell edges (Fig. 3). This means that the number of available sites for exerting traction increases only as the square root of the area times the bond density. Meanwhile, the force per bond is independent of σ, since it is at the limiting maximum value for failure. If one averages force over the entire cell area to obtain traction, the effect of increasing σ is largely counterbalanced by the effect of increasing area.

In the present study, we have observed that $\|A\|$ is an increasing function of the collagen surface density if $\sigma \leq 160\ \mu m^{-2}$, whereas above this level $\|A\|$ becomes a decreasing function. This is most unexpected since previous authors have reported that cell spreading is a monotonic increasing function of surface adhesivity (Mooney et al., 1995). From an abstract perspective, the data surely mean that in our system there is a major qualitative change in the cell-substrate interactions when σ is significantly below or above the transition level of $\sim 160\ \mu m^{-2}$. A hint about the physical basis of this change comes from the fact that the density of integrin receptors on a fibroblast is $\sim 200\ \mu m^{-2}$. Therefore, if σ is increased above the transition threshold, the limiting factor for adhesion is no longer the availability of collagen sites but rather the availability of unattached integrin molecules. Given $\sim 5 \times 10^5$ integrin receptors within the membrane of a fibroblast (Akiyama and Yamada, 1985), the force per bond at very high collagen density becomes only ~ 1.0 pN, which is now safely below the characteristic force needed for rupture of a typical integrin linkage (Lee and Marchant, 2001; Lehenkari and Horton, 1999). This means that the cell-substrate linkages are likely to be very stable and slow to dissociate.

A simple qualitative model to explain why increasing σ under such conditions can decrease $\|A\|$ is illustrated in Fig. 6. At the transition point, the model illustrates that all the integrins on the cell are bound to the substrate. At this point, further spreading is impossible since free integrin receptors are needed at the cell periphery to allow the cell to expand and bind to additional areas of the substrate. If the density of the sites on the substrate is increased beyond the transition point, this saturation of the integrin receptors will occur at a lesser degree of spreading. Thus, the cell spreads less even though the substrate is more adhesive.

This so-called ''receptor saturation'' model was originally proposed and analyzed thermodynamically many years ago by one of the authors (Dembo and Bell, 1987). Among its many predictions is that the overall number of adhesive bonds will indeed continue to increase even while the area of contact goes down. This means that the bound receptors will become clustered in a smaller area at higher and higher densities of ligand. Such clustering of receptors is in many cases associated with cell signaling that activates contraction and motility. For example, this is observed in the phagocytosis of latex beads where a critical density of adhesive sites is needed to activate engulfment (Grinnell and Geiger, 1986). Another example of this sort of signaling occurs in the immune synapse between the antigen presenting cell and the T cell (Grakoui et al., 1999). The possibility of altered signaling at high σ provides an alternative to the mechanically oriented ''receptor saturation'' model as an explanation for our results. In support of this latter view, recent work by Cox et al. (2001) showed that very high surface concentrations of fibronectin activate signals involving integrins and the Rho family of GTPases that inhibit motility and spreading.

Our observations of the relation of collagen ligand density and cell speed are similar to the data reported by DiMilla et al. (1993) for human smooth muscle cells plated on different concentrations of fibronectin and type IV collagen. Population average speed is initially an increasing function of σ when this quantity is not too far above the critical level. However, if σ gets too high, then $\|S\|$ begins to decrease. It is generally accepted that this occurs because the substrate becomes overly adhesive and the contractility of the cell is unable to overcome the adhesive attachments. This is consistent with the receptor saturation model since clustering of bonds makes it easier for them to resist concentrated mechanical loads that promote detachment at the tailing edge of a moving cell. Also in agreement with the saturation model is the fact that traction per unit area is increasing at high ligand density. The added traction is needed because clustering of receptors means that a moving cell needs to disrupt and reform a greater number of bonds for each micron of forward motion.

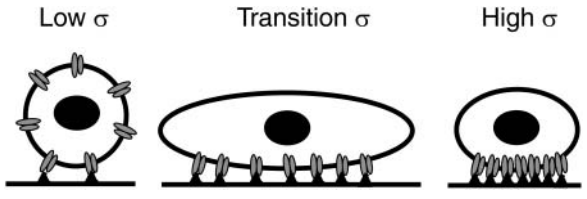

FIGURE 6 Receptor saturation model to explain the dependence of $\|A\|$ of the BALB/c 3T3 fibroblast on σ. At low σ, the number of adhesive sites available to the cell is low, and thus the cell is not able to spread effectively. As σ is increased, $\|A\|$ rises and eventually reaches a maximum at a point where the number of available integrin receptors within the cell is approximately equal to the number of ligand binding sites on the substrata. However, as σ is increased past this point, $\|A\|$ becomes a decreasing function of σ since the integrin receptors become saturated by the ligand on the substrata over a smaller distance.

We thank Xin Brown for the collagen quantitation studies and Andreas Kern for helpful discussions.

This project was supported by the Whitaker Foundation (RG-98-0506) and a National Science Foundation CAREER Award (BES-9985338 to J.Y.W.); the Computational Science Graduate Fellowship Program of the Office of Scientific Computing and Office of Defense Programs in the Department of Energy under contract DE-FG02-97ER25308 (to W.A.M.); and National Institutes of Health grant RO1 GM61806 (to M.D.).

REFERENCES

Akiyama, S. K., and K. M. Yamada. 1985. The interaction of plasma fibronectin with fibroblastic cells in suspension. *J. Biol. Chem.* 260: 4492–4500.

Balaban, N. Q., U. S. Schwarz, D. Riveline, P. Goichberg, G. Tzur, I. Sabanay, D. Mahalu, S. Safran, A. Bershadsky, L. Addadi, and B. Geiger. 2001. Force and focal adhesion assembly: a close relationship studied using elastic micropatterned substrates. *Nat. Cell Biol.* 3:466–472.

Beningo, K. A., M. Dembo, I. Kaverina, J. V. Small, and Y.-L. Wang. 2001. Nascent focal adhesions are responsible for the generation of strong propulsive forces in migrating fibroblasts. *J. Cell Biol.* 153:881–888.

Beningo, K. A., C. M. Lo, and Y.-L. Wang. 2002. Flexible polyacrylamide substrata for the analysis of mechanical interactions at cell-substratum adhesions. *Methods Cell Biol.* 69:325–339.

Carter, S. B. 1967. Haptotaxis and the mechanism of cell motility. *Nature.* 213:256–260.

Cox, E. A., S. K. Sastry, and A. Huttenlocher. 2001. Integrin-mediated adhesion regulates cell polarity and membrane protrusion through the Rho family of GTPases. *Mol. Biol. Cell.* 12:265–277.

Dembo, M., and G. I. Bell. 1987. The thermodynamics of cell adhesion. *In* Current Topics in Membranes and Transport, Vol. 29. F. Bronner and A. Kleinzeller, editors. Academic Press, New York. 71–89.

Dembo, M., T. Oliver, A. Ishihara, and K. Jacobson. 1996. Imaging the traction stresses exerted by locomoting cells with the elastic substratum method. *Biophys. J.* 70:2008–2022.

Dembo, M., and Y. L. Wang. 1999. Stresses at the cell-to-substrate interface during locomotion of fibroblasts. *Biophys. J.* 76:2307–2316.

Dickinson, R. B., and R. T. Tranquillo. 1993. A stochastic model for adhesion-mediated cell random motility and haptotaxis. *J. Math. Biol.* 31:563–600.

Di Lullo, G. A., S. M. Sweeney, J. Korkko, L. Ala-Kokko, and J. D. San Antonio. 2002. Mapping the ligand-binding sites and disease-associated mutations on the most abundant protein in the human, type I collagen. *J. Biol. Chem.* 277:4223–4231.

DiMilla, P. A., K. Barbee, and D. A. Lauffenburger. 1991. Mathematical model for the effects of adhesion and mechanics on cell migration speed. *Biophys. J.* 60:15–37.

DiMilla, P. A., J. A. Quinn, S. M. Albelda, and D. A. Lauffenburger. 1992. Measurement of individual cell migration parameters for human tissue cells. *AIChE J.* 38:1092–1104.

DiMilla, P. A., J. A. Stone, J. A. Quinn, S. M. Albelda, and D. A. Lauffenburger. 1993. Maximal migration of human smooth muscle cells on fibronectin and type IV collagen occurs at an intermediate attachment strength. *J. Cell Biol.* 122:729–737.

Dunn, G. A. 1983. Characterizing a kinesis response: time averaged measures of cell speed and directional persistence. *Agents Actions.* 12(Suppl.):14–33.

Grakoui, A., S. K. Bromley, C. Sumen, M. M. Davis, A. S. Shaw, P. M. Allen, and M. L. Dustin. 1999. The immunological synapse: a molecular machine controlling T cell activation. *Science.* 285:221–227.

Grinnell, F., and B. Geiger. 1986. Interaction of fibronectin-coated beads with attached and spread fibroblasts: binding, phagocytosis, and cytoskeletal reorganization. *Exp. Cell Res.* 162:449–461.

Hansen, L. K., D. J. Mooney, J. P. Vacanti, and D. E. Ingber. 1994. Integrin binding and cell spreading on extracellular matrix act at different points in the cell cycle to promote hepatocyte growth. *Mol. Biol. Cell.* 5: 967–975.

Harris, A. 1973. Behavior of cultured cells on substrata of variable adhesiveness. *Exp. Cell Res.* 77:285–297.

Landau, L. D., and E. M. Lifshitz. 1986. Theory of Elasticity, 3rd ed. J. B. Sykes and W. H. Reid, translators. Pergamon Press, Oxford.

Lee, I., and R. E. Marchant. 2001. Force measurements on the molecular interactions between ligand (RGD) and human platelet α(IIb) β(3) receptor system. *Surf. Sci.* 491:433–443.

Lehenkari, P. P., and M. A. Horton. 1999. Single integrin molecule adhesion forces in intact cells measured by atomic force microscopy. *Biochem. Biophys. Res. Commun.* 259:645–650.

Li, Y., Z. Hu, and C. Li. 1993. New method for measuring Poisson's ratio in polymer gels. *J. Appl. Polym. Sci.* 50:1107–1111.

Lo, C. M., H. B. Wang, M. Dembo, and Y.-L. Wang. 2000. Cell movement is guided by the rigidity of the substrate. *Biophys. J.* 79:144–152.

Marganski, W. A., M. Dembo, and Y.-L. Wang. 2003. Measurements of cell-generated deformations on flexible substrata using correlation-based optical flow. *Methods Enzymol.* 361:197–211.

Mooney, D., L. Hansen, J. Vacanti, R. Langer, S. Farmer, and D. Ingber. 1992. Switching from differentiation to growth in hepatocytes: control by extracellular matrix. *J. Cell. Physiol.* 151:497–505.

Mooney, D. J., R. Langer, and D. E. Ingber. 1995. Cytoskeletal filament assembly and the control of cell spreading and function by extracellular matrix. *J. Cell Sci.* 108:2311–2320.

Munevar, S., Y.-L. Wang, and M. Dembo. 2001a. Traction force microscopy of migrating normal and H-ras transformed 3T3 fibroblasts. *Biophys. J.* 80:1744–1757.

Munevar, S., Y.-L. Wang, and M. Dembo. 2001b. Distinct roles of frontal and rear cell-substrate adhesions in fibroblast migration. *Mol. Biol. Cell.* 12:3947–3954.

Palecek, S. P., J. C. Loftus, M. H. Ginsberg, D. A. Lauffenburger, and A. F. Horwitz. 1997. Integrin-ligand binding properties govern cell migration speed through cell-substratum adhesiveness. *Nature.* 385:537–540.

Pelham, R. J., and Y.-L. Wang. 1997. Cell locomotion and focal adhesions are regulated by substrate flexibility. *Proc. Natl. Acad. Sci. USA.* 94: 13661–13665.

Tan, J. L., J. Tien, D. M. Pirone, D. S. Gray, K. Bhadriraju, and C. S. Chen. 2003. Cells lying on a bed of microneedles: an approach to isolate mechanical force. *Proc. Natl. Acad. Sci. USA.* 100:1484–1489.

Walsh, B. J., S. C. Thornton, R. Penny, and S. N. Breit. 1992. Microplate reader-based quantitation of collagens. *Anal. Biochem.* 203:187–190.

Wang, H. B., M. Dembo, S. K. Hanks, and Y.-L. Wang. 2001. Focal adhesion kinase is involved in mechanosensing during fibroblast migration. *Proc. Natl. Acad. Sci. USA.* 98:11295–11300.

Wang, Y.-L., and R. J. Pelham. 1998. Preparation of a flexible, porous polyacrylamide substrate for mechanical studies of cultured cells. *Methods Enzymol.* 298:489–496.

Wong, J. Y., A. Velasco, P. Rajagopalan, and Q. Pham. 2003. Directed movement of vascular smooth muscle cells on gradient-compliant hydrogels. *Langmuir.* 19:1908–1913.